

From avalanches to fluid flow: A continuous picture of grain dynamics down a heap

P.-A. Lemieux and D. J. Durian

UCLA Department of Physics & Astronomy, Los Angeles, CA 90095-1547

(November 16, 2018)

Surface flows are excited by steadily adding spherical glass beads to the top of a heap. To simultaneously characterize the fast single-grain dynamics and the much slower collective intermittency of the flow, we extend photon-correlation spectroscopy via fourth-order temporal correlations in the scattered light intensity. We find that microscopic grain dynamics during an avalanche are similar to those in the continuous flow just above the transition. We also find that there is a minimum jamming time, even arbitrarily close to the transition.

45.70.-n, 83.70.Fn, 42.50.Ar, 07.50.Qx

We have all poured sand in a heap. If grains are added rapidly, the heap relaxes through continuous, fluid-like flow at its surface. If grains are added slowly, it relaxes intermittently through discrete avalanches. The existence of both continuous and intermittent regimes is characteristic of the dual nature of granular media, which can exhibit properties of both liquids and solids [1,2]. Similar behavior, such as bubble rearrangements in foams or kinetic heterogeneities in supercooled liquids, arises in other systems near the onset of jamming [3,4]. In spite of its ubiquity, and its obvious importance for applications and geophysical phenomena, the transition between intermittent and continuous flow has received relatively little attention. One reason may be that kinetic theories [5,6] of granular hydrodynamics, as well as minimal-ingredient theories of surface behavior [7], apply only to continuous flows, while cellular-automata models of avalanches apply only to rate-independent intermittent flows [8]; both approaches break down near the transition. Another reason may be the vast separation in time scales between the grain velocity fluctuations and the intermittency dynamics, which makes it difficult to capture both phenomena simultaneously.

Recently we used diffusing-wave spectroscopy (DWS), a photon-correlation spectroscopy for opaque media [9], to probe motion in homogeneously excited sand [10]. DWS reveals dynamics on time- and length-scales too small for imaging, but cannot be applied to intermittent flows. This is because in the static periods all the grains are perfectly correlated, violating the assumption that the total scattered electric field has Gaussian statistics. Here, for a heap upon which grains are steadily poured, we show how intermittency can be detected and characterized using higher-order temporal correlations in the intensity of multiply-scattered laser light. We extract single-grain dynamics, as well as probability functions describing the collective intermittency of the flow. This gives an unprecedented picture of the dynamics in both intermittent and continuous flows, as well as across the transition between these extremes.

System. The experimental setup (Fig. 1a) consists of parallel static-dissipating plastic walls, 30x30 cm², form-

ing a $w = 9.5$ mm wide vertical channel closed at the bottom and on one side. We use spherical glass beads of diameter 0.33 ± 0.03 mm, large enough to minimize effects of interstitial gas and electrostatic forces while keeping the system size manageable; the density of the packing is $\rho = 1.35$ g/cc. Flow is created by dropping grains into the closed side of the channel, and breaking their fall by a secondary hopper just above the heap. Grains falling out the open end are recycled by a vacuum-driven elevator. The flow rate is set by a micrometer-controlled gate valve and a knife-edge, allowing for wide variation of 0.025-5 g/s (50-10,000 grains/s). Prior to a run, the beads are washed, dried in air, and circulated until a steady state is reached.

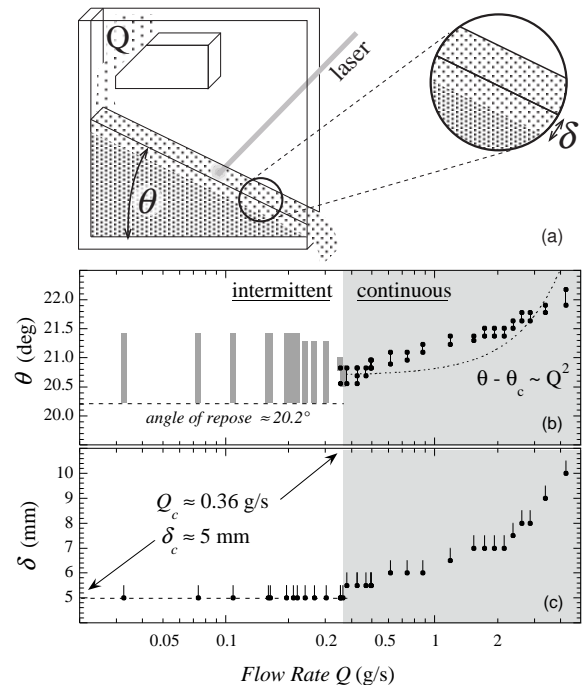


FIG. 1. The experimental setup (a), and two macroscopic measures of the response vs mass flow rate: (b) heap angle and (c) layer thickness.

For orientation the macroscopic behavior of the heap is summarized in Figs. 1b-c vs mass flow rate, Q , the sole parameter that sets the grain dynamics. As opposed to the inclined-plane geometry [11], our system chooses both the angle θ of the heap and the thickness δ of the flowing layer. This avoids such issues as the role of the plane roughness, and should ultimately permit more direct contact with theory. Visual inspection reveals that the transition between intermittent and continuous flows is at $Q_c = 0.36$ g/s, and that it is rather sharp. By contrast with the rotating-drum geometry [12,13], this transition is not hysteretic [13], and avalanches always start at the top. Also by contrast, both δ and θ are uniform across the whole surface. Fig. 1 shows that these quantities become independent of Q in the intermittent regime, with θ ranging between a minimum angle of repose and a maximum angle of stability, and with δ being the same thickness as at the transition, $\delta_c = 5$ mm, which is about 15 grain diameters or about half the width of the channel. Thinner layers cannot flow indefinitely, as dissipative forces overwhelm gravity and inertia. Fig. 1 also shows how both θ and δ increase monotonically for continuous flows above the transition. Interestingly, the heap angle varies logarithmically with Q and, as measured at the walls for $Q = 0.5$ g/s, the velocity vs depth is nearly exponential, $v_x(z) \approx (1 \text{ cm/s}) \exp[-z/(0.15 \text{ cm})]$ for $z < \delta$ [14]. This is unlike the modified-Bagnold model predictions of $\theta - \theta_c \propto Q^2$ and $v_x(z) \propto (\delta^{3/2} - z^{3/2})$ [13]. This implies that there must be enduring contacts and/or that the rate of collisions is not set by dv_x/dz .

Light Scattering. While visual measurements provide a rough overview of a heap's macroscopic response, multiple-light scattering measurements provide a detailed picture of both individual and collective grain dynamics over a broad range of time scales. Here we illuminate the top surface with an Ar^+ laser, wavelength $\lambda = 514$ nm, over a 8 mm region located $L = 18$ cm from the closed end. The intensity fluctuations in the speckle pattern created by backscattered photons are captured by a single-mode optical fiber coupled to a photon-counting assembly. Following Ref. [15], we measure simultaneously in real-time both the second- and fourth-order intensity correlation functions $g^{(2)}(\tau) = \langle I(0)I(\tau) \rangle / \langle I \rangle^2$ and $g_T^{(4)}(\tau) = \langle I(0)I(T)I(\tau)I(\tau+T) \rangle / \langle I \rangle^4$, where T is a fixed delay that can be chosen between 50 ns and 50 ms, and τ is swept over a range of values by a digital correlator. In analogy with the 'second-spectrum' [16], $g_T^{(4)}(\tau)$ can be thought of as a 'second-correlation' or 'correlation of correlation' quantifying fluctuations in the correlation signal $I(t)I(t+T)$ with time t .

Examples of $g^{(2)}(\tau)$ and $g_T^{(4)}(\tau)$ are shown in Fig. 2. For continuous flows, both correlations exhibit a single complete decay at short time scales. Good agreement is seen between $g_T^{(4)}(\tau)$ data and the predictions generated solely from $g^{(2)}(\tau)$ data, as in Ref. [15], showing that the fluctuations are Gaussian. Therefore, the usual machinery of DWS may be applied to extract single-grain

dynamics. For intermittent flows, by contrast, both correlations exhibit a partial decay at short times, followed by a plateau and a final decay at long times. Furthermore, the fluctuations are non-Gaussian, implying that a new model is required to extract grain motion.

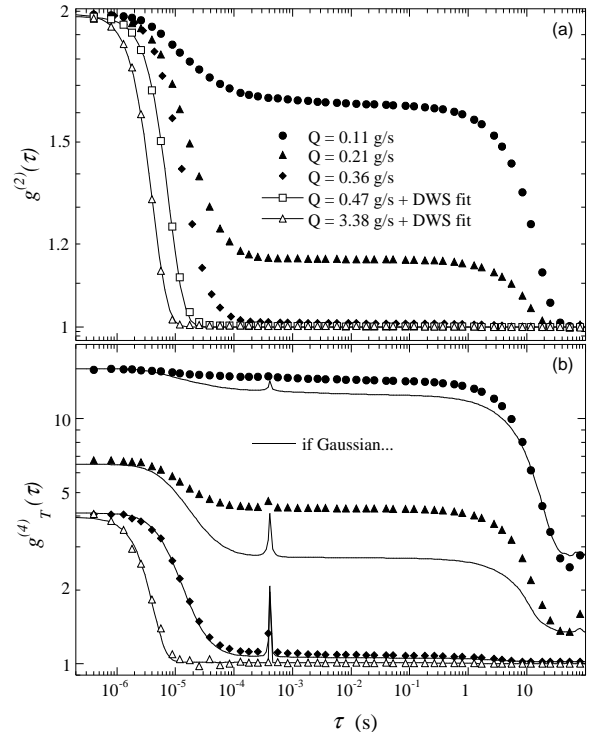


FIG. 2. Examples of (a) second- and (b) fourth-order temporal correlations in the intensity of laser light multiply-scattered from the surface of the heap. For continuous flows, the fluctuations are Gaussian and the correlations exhibit a single decay; for intermittent flows, the fluctuations are non-Gaussian and the correlations exhibit a two-step decay.

Several ingredients are required to model the full spectrum of grain dynamics. One is the usual normalized electric field autocorrelation function $\gamma(\tau)$, whose Fourier transform gives the broadening of the power spectrum due to relative motion of scattering sites during flow. For our backscattering geometry, the theory of DWS [9,17] gives $|\gamma(\tau)| \propto \exp[-2\sqrt{k^2\delta v^2\tau^2 + 3l^*/l_a}]$, where $k = 2\pi/\lambda$, δv is a typical relative grain speed averaged over the scattering volume, $l^* = 1.3$ mm is the photon transport mean-free path, and $l_a = 1.0$ cm is the photon absorption length. Since δv is the only quantity not known in advance, it may be extracted from the data.

All other ingredients relate to the probabilities with which the system switches between flowing / '1' and static / '0' states. Most important is the probability $P_0(\tau)$ for the system to be in the *same* static configuration after a time interval τ . This function decays monotonically from one to zero. It can be related to the probability $P(\tau)$ that two flowing states are separated by τ via $P_0(\tau) = \int_\tau^\infty \tilde{P}(\tau')(\tau' - \tau)d\tau'/t_0$, and hence by

$\tilde{P}(\tau) = t_0 d^2 P_0 / d\tau^2$, where t_0 is the average static state duration. Also important are the probabilities $P_{ij}(\tau)$ for the system, if initially in state i , to be in state j after a time τ . These interrelated functions decay from either 1 or 0 to the fraction of time f_j spent in state j .

Making the simplest assumption consistent with visual observations, that starting/stopping transients are negligible and that the speckle pattern fluctuates rapidly during each flowing state but is constant during each static state, we find

$$g^{(2)}(\tau) = 1 + \beta [f_1 P_{11}(\tau) |\gamma(\tau)|^2 + f_0 P_0(\tau)], \quad (1)$$

where $1/\beta$ is roughly the number of speckles viewed by the detector. For continuous flow, where f_1 and P_{11} are identically one, Eq.(1) reduces to the usual Siegert relation connecting intensity and field autocorrelations. For intermittent flow, Eq.(1) exhibits a decay at short times due to $\gamma(\tau)$, during which the switching functions are constant, and a final decay at long times due to $P_0(\tau)$. This is unlike the two-step decay seen in supercooled systems, where the field fluctuations are Gaussian and the final decay (the α -relaxation) is due to cage-hopping effects. Note that the intercept $g^{(2)}(0) = 1 + \beta$ gives the same second intensity moment as for a Gaussian process; this property also holds in our general expressions for $g^{(3)}$ and $g^{(4)}$. Intermittency gives non-Gaussian fluctuations because of *grain correlations* during each static state, unlike the broader intensity distributions familiar from number fluctuations in single-scattering experiments.

The predictions for higher-order correlations are cumbersome, but reduce considerably for the usual case of good separation in decay scales for $\gamma(\tau)$ and the switching functions. Choosing an intermediate value for the fixed delay T , so that $\gamma(T) = 0$ and $P(\tau \pm T) = P(\tau)$, we find

$$g_T^{(4)}(\tau) \approx 1 + \beta f_1 [2 + \beta |\gamma(\tau)|^2] |\gamma(\tau)|^2 + \beta f_0 [2 + \beta P_{00}(t) + (4 + 10\beta + 6\beta^2) P_0(t)]. \quad (2)$$

This neglects terms in $\gamma(|\tau - T|)$, which cause a peak in $g_T^{(4)}(\tau)$ at $\tau = T$ that is characteristic of our slice of the full $g^{(4)}(\tau_1, \tau_2, \tau_3)$. As above, Eq.(2) exhibits a single decay for continuous flows and a two-step decay for intermittent flows. Armed with Eqs. (1-2), one can not only reliably detect the presence of intermittency, but can also characterize both the grain motion via $\gamma(\tau)$ and the collective intermittency of the flows via $P_0(\tau)$ and $P_{ij}(\tau)$. This extends the utility of photon-correlation techniques (not just DWS) to systems like slowly-driven sand exhibiting intermittency.

Grain Dynamics. For continuous flows, according to the above discussion, the correlations fully decay at a time scale given approximately by $\lambda/\delta v$. Using δv as the sole parameter, we obtain excellent fits to $g^{(2)}(\tau)$ (and equivalently to $g_T^{(4)}(\tau)$ since here the fluctuations are Gaussian) as shown in Fig. 2(a). The results in Fig. 3(a) show that δv varies logarithmically with the flow rate,

just like the heap angle. The value of δv appears to reflect both shear flow and random ballistic motion. At $Q = 0.5$ g/s, slightly above the transition, the r.m.s. average strain rate in the scattering volume is estimated from $v_x(z)$ and Q to be less than 4/s. This gives a contribution to δv of $l^* \sqrt{\langle \dot{\gamma}^2 \rangle} / 5 = 0.4$ cm/s [17], which accounts for half the fitted value of 0.8 cm/s. We believe that the random contribution is not due to free-flight between grain-grain collisions, since the Bagnold model does not apply, but is rather due to jostling parallel and perpendicular to the average flow as shearing layers slide over one another with grains always maintaining a near close-packing arrangement. While there is no saltation, altered dynamics at the free surface may also contribute. In any case, the extracted values of δv represent a measure of microscopic velocity fluctuations for the flowing grains. These are related to the average flow speed as $\delta v \sim v^{0.5 \pm 0.1}$, similar to previous observations for a vertical hopper [10]. The increase of fluctuations relative to the average may be the ultimate cause of jamming at low driving rates.

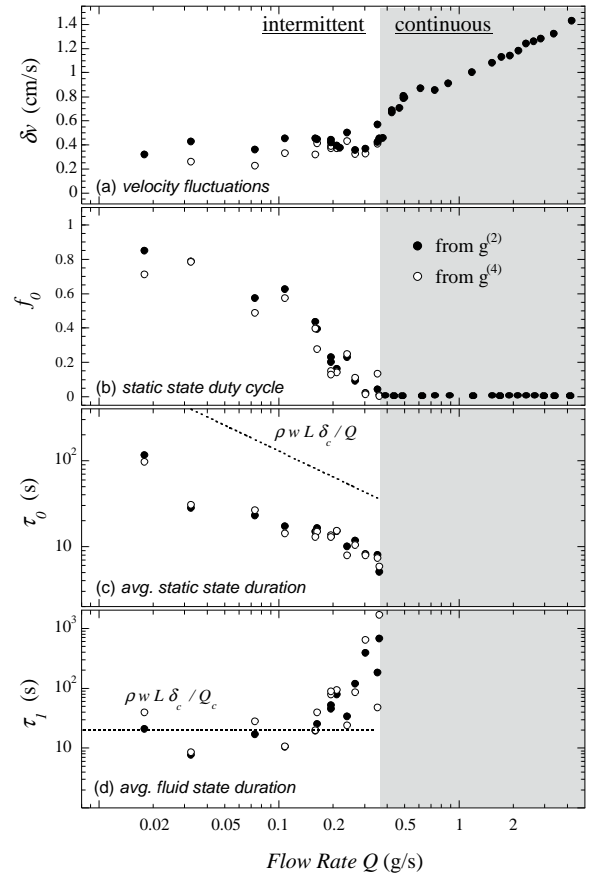


FIG. 3. Grain dynamics vs mass flow rate: (a) velocity fluctuations, (b) fraction of time spent static, (c) average time spend static, and (d) average time spend flowing. Consistent results are obtained from second- and fourth-order correlation data using Eqs.1 and 2, respectively.

For intermittent flows, according to the light scatter-

ing discussion, the correlations partially decay at $\lambda/\delta v$ and then fully decay at a time scale reflecting the intermittency dynamics. Eqs. (1-2) show that between these decays the correlations plateau at values of $1 + \beta f_0$ and $1 + \beta(6 + 11\beta + 6\beta^2)f_0$, respectively. Knowing $\beta \approx 1$, we easily extract the fraction of time f_0 the system spends at rest. The results in Fig. 3(b) show that the $g^{(2)}(\tau)$ and $g_T^{(4)}(\tau)$ plateaus are consistent and in accord with expectations. As the flow rate goes to 0 (Q_c), f_0 approaches 1 (0), denoting a completely static (fluid) state.

Given the correlation plateaus, we may also fit the early-time decay for grain-scale velocity fluctuations *during* avalanches using Eqs.(1-2). The results in Fig. 3(a) show that δv is approximately independent of Q in the intermittent regime. Furthermore, the value is close to, but perhaps slightly less than, that for fluctuations in continuous flow just above the transition. So avalanches are not very different from barely-continuous flow.

Finally we analyze the late-time decay of the intensity correlations in terms of avalanche statistics. Specifically, the functional form of the the switching function $P_0(\tau)$ may be deduced from $g^{(2)}(\tau)$ data using Eq.(1) and the known plateau values. Similarly $P_0(\tau)$ may be deduced from $g_T^{(4)}(\tau)$ data, ignoring the small contribution in Eq.(2) from $P_{00}(\tau)$. The two results agree, and for all Q are consistent with the empirical form $P_0(\tau) = \exp(-\tau/t_0)/[1 + (\tau/t_0)^2/2]$. Namely, the first half of the decay is linear, and the second half is faster than exponential. This rules out self-organized criticality, for which $P_0(\tau)$ would be a power-law, as well as random-telegraph switching, for which $P_0(\tau)$ would be perfectly exponential. Rather, the distribution of intervals between avalanches is peaked around an average, t_0 , similar to behavior seen in Ref. [12].

Results for the average static and flowing times, deduced respectively from $P_0(\tau) = 1 - \tau/t_0 + \dots$ and $f_0 = t_0/(t_0 + t_1)$, are shown in Fig. 3(c-d) as a function of flow rate. For the smallest Q , we find evidence of a quasi-static limit in which the time between avalanches scales as $1/Q$ and in which the duration of avalanches t_1 approaches a constant. The observed times are on the order of the upper limits $\rho w L \delta_c / Q$ and $\rho \delta_c w L / Q_c$ needed to fill and to empty, respectively, a volume $w L \delta_c$ of sand above the illumination spot. As the flow rate is increased toward Q_c , where continuous flow commences, the time spent flowing appears from Fig. 3(d) to diverge. Interestingly, at the same point, the time spent in the static state does not vanish continuously but rather approaches a nonzero constant. Even arbitrarily close to smooth flow, it takes significant time for the system to start moving again after it has jammed. This is analogous to common experience on a freeway, where traffic jams develop very suddenly but clear much more slowly.

Conclusions. In summary we have introduced a novel optical method and used it to probe, simultaneously, both avalanche statistics and microscopic grain dynamics *within* the avalanches. A unique feature is that the tech-

nique applies to both continuous and quasi-static intermittent flows, as well as to the transition between these extremes. This should enable a wide range of new experiments on granular dynamics as a high driving rate of tumbling, shaking, blowing, sprinkling, shearing, etc., is decreased and the system develops intermittent dynamics as a precursor to complete jamming. For example we are currently investigating the influence of channel dimensions, and the behavior as a function of depth, for the sprinkling geometry presented here. The results should help guide and test fundamental theories of granular flow that are based on the actual microscopic grain dynamics.

This work was supported by NSF grant DMR-0070329.

-
- [1] H.M. Jaeger, S.R. Nagel, and R.P. Behringer, *Rev. Mod. Phys.* **68**, 1259 (1996).
 - [2] J. Duran, *Sands, Powders, and Grains: An Introduction to the Physics of Granular Materials* (Springer, NY, 1999).
 - [3] M.E. Cates, J.P. Wittmer, J.P. Bouchaud, and P. Claudin, *Phys. Rev. Lett.* **81**, 1841 (1998).
 - [4] A.J. Liu and S.R. Nagel, *Nature* **396**, 21 (1998).
 - [5] J.T. Jenkins and S.B. Savage, *J. Fluid Mech.* **130** 187 (1983).
 - [6] P.K. Haff, *J. Fluid Mech.* **134** 401 (1983).
 - [7] P. Bouchaud, M.E. Cates, J.R. Prakash, and S.F. Edwards, *J. de Phys. I* **4**, 1383 (1994).
 - [8] P. Bak, C. Tang, and K. Wiesenfeld, *Phys. Rev. A* **38**, 364 (1988).
 - [9] D.A. Weitz and D.J. Pine in *Dynamic Light Scattering: The Method and Some Applications*, edited by W. Brown (Clarendon Press, Oxford, 1993) pp. 652-720; G. Maret, *Curr. Op. Coll. I. Sci.* **2** 251 (1997).
 - [10] N. Menon and D.J. Durian, *Science* **275**, 1920 (1997); *Phys. Rev. Lett.* **79**, 3407 (1997).
 - [11] O. Pouliquen, *Phys. Fluids* **11**, 542 (1999).
 - [12] H.M. Jaeger, C.-h. Liu, S.R. Nagel, *Phys. Rev. Lett.* **62**, 40 (1989).
 - [13] J. Rajchenbach, *Phys. Rev. Lett.* **65**, 2221 (1990).
 - [14] An exponential profile occurs if viscosity scales inversely with strain rate, *e.g.* due to a yield stress; in the Bagnold model, viscosity is proportional to strain rate. We note that $\int \rho v_x(z) w dz$ gives only $0.4Q$, showing that grains do not slip freely along the vertical walls of the channel.
 - [15] P.-A. Lemieux and D.J. Durian, *J. Opt. Soc. Am A* **16**, 1651 (1999).
 - [16] M.B. Weissman, *Annu. Rev. Mater. Sci.* **26**, 395 (1996).
 - [17] X.-l. Wu, D.J. Pine, P.M. Chaikin, J.S. Huang, and D.A. Weitz, *J. Opt. Soc. Am. B* **7**, 15 (1990).